Code Division Positioning by Continuous Signals Using Spread Spectrum Ultrasonic Waves

Ken Kumakura and Akimasa Suzuki and Taketoshi Iyota
Soka University
1-236, Tangi-machi, Hachioji, Tokyo, Japan
e-mail: e12m5206@soka.ac.jp

Abstract—**Indoor real-time positioning is required in order to realize self-localization for autonomous mobile robots. In particular, accurate control in plural mobile robots requires 3-D coordinate information. This paper presents the positioning accuracy and response time for a 3-D real-time indoor positioning system which uses continuous spread spectrum ultrasonic signals that are generated and detected using inexpensive all-purpose transducers, and a Code Division Multiple Access (CDMA) communication system. For application with moving targets, we propose signal acquisition and tracking using continuous signals in analogy to the already effective Global Navigation Satellite System (GNSS). The proposed calculation algorithm for coordinate acquisition is based on the Newton-Raphson method for continuous signals. The calculation time and accuracy of this method is verified by conducting a positioning experiment. The results show that the positioning error is less than 50 mm in a 4000 mm by 4000 mm experimental space with 4 transmitters. Moreover, the maximum response time to update a result is 80 ms, displaying the efficacy of this system for robot navigation.**

Keywords-component; Spread Spectrum Signal, Ultrasonic Waves, Real-time Indoor Positioning, CDMA, Newton-Raphson Method

I. INTRODUCTION

Autonomous mobile robots which require self-localization have been actively researched recently. In order to realize self-localization, indoor real-time positioning is required. In particular, the coordinates is required to realize the self-localization of autonomous mobile robots for human-robot symbiosis such as cooperative working between robots and humans. In these cases, the moving targets have to be continuously measured with high accuracy. The positions of each target have to be also identified. Therefore, positioning systems that provide coordinates using infrastructure such as pseudolites [1] or radio waves [2] have been investigated. When compared to other methods, the use of ultrasonic waves is inexpensive and highly accurate [3], and robust to occlusion and illumination changes. However, these systems have weak noise resistance and take a longer period of time to acquire data because the use of Time Division Multiple Access (TDMA) with on-off keying becomes cumbersome as the number of objects being measured increases. Spread spectrum (SS) ultrasonic waves have been investigated [4] to overcome this.

Previously, we have also proposed an inexpensive and accurate real-time 3-D positioning system with SS ultrasonic signals, using an all-purpose transducer, low-power Field-Programmable Gate Array (FPGA), and a small microprocessor. Previous studies on the component technologies of this system such as the Code Division Multiple Access (CDMA) [5], measurement precision of all-purpose transducers [6], and the positioning accuracy considering the Delusion of Precision [7] have been discussed in offline processing. We have also investigated a real-time hardware computation for correlation calculations [8]. Further, the effectiveness of the use of signal acquisition and tracking using a continuous signal (analogous to the Global Navigation Satellite System (GNSS)) has been shown [9]. In this system the number of reception units is not limited; position and direction information for an unspecified number of targets can be obtained at the same time. In addition, communication between environments and positioning targets is not required. This allows for self-localization to be achieved without endangering the privacy of the user.

This requires continuous calculation of the positioning coordinate using continuous signals. However, real-time code division positioning using continuous signals has not been experimentally achieved to date. We propose the calculation of an algorithm based on the Newton-Raphson method for continuous signals, and present the positioning accuracy and response time from our real-time experiments. Positioning errors of less than 50 mm in a 4000 mm by 4000 mm space with 4 transmitters were obtained. A maximum response time of 80 ms was found when updating a position. We show that sufficient positioning accuracy is achieved in our real-time calculations.

II. GENERATION AND DETECTION OF SS SIGNALS

A. Generation Method of MLS

SS ultrasonic waves were generated using a Maximum Length Sequence (MLS). MLS is a pseudo-random code sequence, which consists of "0" and "1", and this sequence is obtained easily from a shift register in FPGA. The bit length of this shift register governs the calculation result and signal to noise ratio. In our system, a 9-bit shift register was utilized to achieve real-time correlation calculations with a high S/N ratio. Fig. 1 presents the logic which generates the MLS

978-1-4799-4043-1/13/$31.00

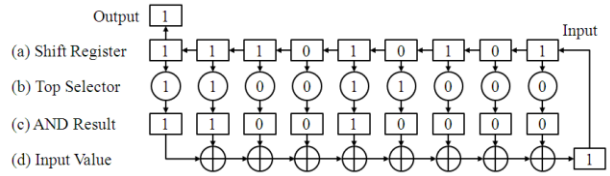

Fig. 1 Logic for generating MLS by using a 9-bit shift register

using a 9-bit shift register. Fig. 1 (a) to (d) show the values of the shift register, the value of the tap selector, the result of the AND operation, and the input value to the shift register, respectively.

During the first operation the initial value in Fig. 1 (a) is input to each bit of the shift register. Using contained values, a tap-selector is prepared to decide the next input value to the shift register (see Fig. 1 (b)). The value in Fig. 1 (b) corresponds to MLS. In Fig. 1 (c), the result of the AND operation between Fig. 1 (a) and (b) is output. The result of the exclusive-OR (see Fig. 1 (d)), calculated from the selected value (see Fig. 1 (c)), is used as input for the Least Significant Bit (LSB) of the shift register (see Fig. 1 (a)). After each bit of the shift register is shifted left by one bit and the value in Fig. 1 (d) is input to LSB, the Most Significant Bit (MSB) of the shift register is output. MSB outputs one after another by this hardware becomes MLS. The MLS which is obtained from a 9-bit shift register has 2 bits (chips) periods.

B. SS Signal Modulation and Acquisition with MLS

An SS signal is modulated using carrier waves and MLS in a transmission unit. Fig. 2 shows the modulation and acquisition of an SS signal. In Fig. 2 (a) 1 period of carrier waves is denoted as t_{cr}. Here, we replace the "0" values of the MLS with a "-1" in order to facilitate signal processing in

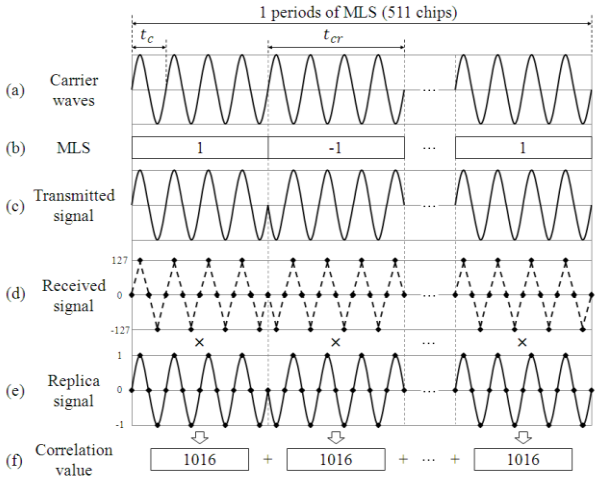

Fig. 2 A SS signal which is generated in the transmission unit and a correlation value, which is calculated in the reception unit. (c) A transmitted signal is formed from multiplication of (a) a carrier waves and (b) a MLS. (f) A correlation value is calculated from the product-sum operation of (d) a received signal and (e) a replica signal in reception unit

Fig. 2 (b). The transmitted signal is generated by multiplying 4 carrier waves and 1 period of MLS, as shown in Fig. 2 (c). If MLS is "-1", the SS signals phase is inverted by 180 degrees. The length of the transmitted signal equals the MLS period (511 t_c). A reception unit calculates the correlation values in order to detect the time of arrival. In Fig. 2 (d), each dot signal indicates a sampling; the number of samples in 1 period of the received signal is selected to be 4 samples. The replica signal in Fig. 2 (e) is the same as the transmitted signal but is generated by a reception unit. The correlation value in Fig. 2 (f) is calculated using a product-sum operation of the received and replica signal for 1 cycle of MLS. In order to detect the transmitted signal, the correlation values are calculated for each sample.

Fig. 3 shows detection of a SS signal and a Time of Flight (TOF) calculation. The vertical and horizontal axes correspond to the correlation values and elapsed time, respectively. The peaks of the correlation values in Fig. 3 are obtained from the self-correlation characteristic of MLS when the phase and frequency of the received signal match that of the replica signal. If the phase and frequency of the received signal deviate from the replica signal, the correlation value becomes very low compared with the peaks in Fig. 3. Here, t_i is defined as the time between the transmission timing of an SS signal that is notified by a transmitter and a peak. Thus, t_i is the TOF of the SS signal between transmitter and receiver. The distance from a transmitter to a receiver is obtained by the TOF and speed of sound in gas. The distance defined as d, is approximated by

, (1)

where T is the temperature [10]. The SS signals obtained from MLS with low cross-correlation have little effect on each other except for near-far resistant; it is possible to simultaneously measure distance with the SS signals. That is transmitters continuously transmit signals without TDMA.

III. Synchronization between a Transmission Unit and a Reception Unit

A. Synchronization of a Sampling Frequency

Sampling frequencies are calculated from the operating frequencies obtained from a crystal oscillator mounted on the transmission and a reception unit. The operating frequencies

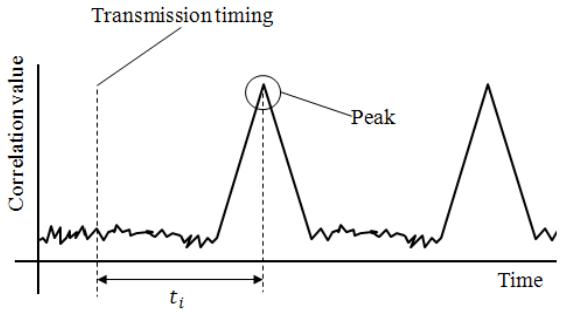

Fig. 3 The signal detection and calculation of TOF for measuring a distance

of each transmission and reception unit are slightly varied by temperature and voltage. A difference in the sampling frequency arises from differences in these operating frequencies. The difference in sampling frequency causes a decrease in the correlation value. Thus, both sampling frequencies must be synchronized for signal detection.

Accurate clock division is used to synchronize the sampling frequency. Using this method, we can divide an operating frequency by any integer or non-integer. The frequency ratio r is given by

—, (2)

where and f_x are the operating and sampling frequencies, respectively. Defining and as the integer part of in (2) and the ratio between and r,

—. (3)

From (2) and (3) f_x is given by

———. (4)

The reception unit measures the difference in operating frequency using an electrical signal at fixed intervals. The operating frequency is measured using a counter as follows. Fig. 4 shows the difference in counted values caused by the sampling frequency difference, where the horizontal axis corresponds to counted values. The transmission unit counts to a constant time interval using the operating frequency and sends notification of timing (i) and (ii) to a reception unit via an electrical signal.

The counter in the reception unit continues incrementing during the timing interval defined by the operating frequency in Fig. 4 (b), such that Fig. 4 (a) and Fig. 4 (b) are matched. As the operating frequency increases, the number of counted values increases, and the operating frequency between the transmission and reception units r_{gap} is:

—, (5)

where s_{mea} and s_{tar} are the measured and target counted values, respectively in Fig. 4. Using (4) and (5), the sampling frequency that is synchronized to the frequency of the transmission unit f_{smp} is

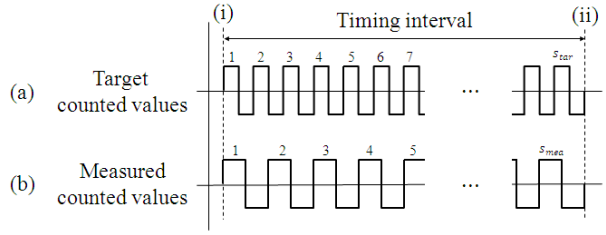

Fig. 4 The conception diagram of difference of counted values by difference of operating frequency in a receiver unit

(———). (6)

B. *Timing Synchronization for Starting Transmission*

In addition to the sampling frequency, the time of transmission is required for synchronized acquisition of TOF. This synchronization is achieved using an electrical signal, as shown in Fig. 5. Defining the time at the start of transmission as k periods in Fig. 5 (a), when a shift register (see Fig. 1 (a)) reaches an arbitrary value ("111111111" in binary in our system) the transmission start timing has a periodicity. This arises from the periodicity of the MLC in Fig. 5(b). Using this periodicity, an electrical signal notifies the transmission start time so that the system is synchronized.

IV. Positioning Calculation Algorithm Based on Newton-Raphson Method

More than 3 distances are required to measure a position since there are 3 coordinates (x, y, z) that must be calculated. Thus, more than 3 transmitters are required, each generating different MLS codes with low cross-correlation, allowing for division positioning. Coordinates on a receiver are calculated from simultaneous equations of the different distances and the known coordinates of the transmitters. We could use a repetitive Newton-Raphson method to solve these equations in analogy to GNSS [11]; however the clock bias term can be removed from the positioning calculation because the proposed system calculates TOF using timings sent by the transmitter.

Our indoor positioning system calculation is outlined in Fig. 6. A target position Rx is calculated from the coordinates of 3 transmitters (Tx_1, Tx_2, and Tx_3) and the distances obtained from the TOFs. A distance, r_i (r_1, r_2, and in Fig. 6) between $\mathrm{Tx}_i(x_i, y_i, z_i)$ and $\mathrm{Rx}(x, y, z)$ is

$\sqrt{(}$, (7)

where $\mathrm{Rx}(x, y, z)$ and $\mathrm{Tx}_i(x_i, y_i, z_i)$ are defined as the true coordinates of a receiver, and the i-th arbitrary coordinates of a transmitter, respectively. The subscript i denotes the transmitter number and takes values 1, 2, ..., n, where n is greater than 3. We write $\mathrm{Rx}(x, y, z)$ as

x, (8)

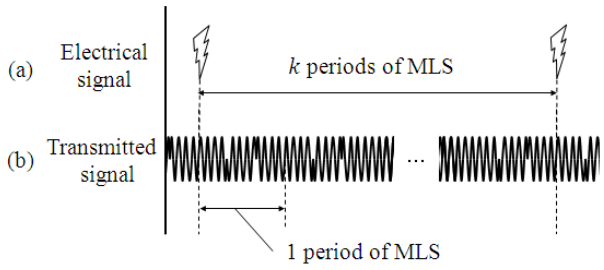

Fig. 5 The conception diagram of method of notices transmission start timing by electrical signal

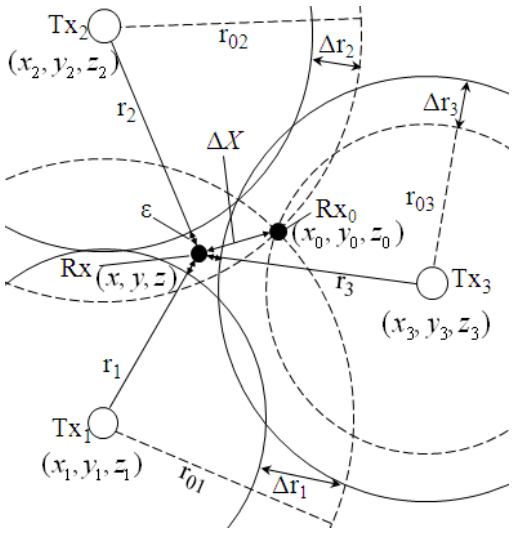

Fig. 6 Diagram for explanation of positioning calculations

y, (9)

z, (10)

where $\mathrm{Rx}_0(x_0, y_0, z_0)$ are the initial coordinates which the positioning system gives. Δx, Δy, Δz are the x, y and z components of correction distance between the initial coordinates and $\mathrm{Rx}_0(x_0, y_0, z_0)$, respectively. The distance between the initial coordinates and the i-th transmitter is

$= \sqrt{(x}$. (11)

Thus the distance between and is given by

. (12)

Partial differential coefficients α_i, β_i and γ_i can be evaluated from Δr_i and the x, y, and z components of $\mathrm{Rx}_0(x_0, y_0, z_0)$, respectively. Δr_i can be also expressed as (13) using α_i, β and γ_i:

$$\begin{pmatrix} \vdots \end{pmatrix} = \begin{pmatrix} \end{pmatrix}\begin{pmatrix} \Delta y \end{pmatrix}. \quad (13)$$

We define a vector R, matrix A, vector X, and vector

$$\begin{pmatrix} \vdots \end{pmatrix}, \quad (14)$$

$$\begin{pmatrix} \end{pmatrix}, \quad (15)$$

$$\begin{pmatrix} \Delta y \end{pmatrix}, \quad (16)$$

$$\begin{pmatrix} \vdots \end{pmatrix}, \quad (17)$$

where ε is the vector of measurement errors. Equation (13) can be denoted by

(18)

using (14), (15), (16) and (17). Let us consider the solution such that the minimum value of ε is obtained using a least squares method [12]. The sum of ε squared, defined as f, is

$$\sum \varepsilon \quad (19)$$

ΔX.

In order to minimize f the partial differential of (19) is carried out with respect to X,

— 0. (20)

The location of extrema is calculated using (20).

A. (21)

is obtained by deformation of (21).

R. (22)

Thus, is:

X. (23)

When $\mathrm{Rx}_0(x_0, y_0, z_0)$ is close to $\mathrm{Rx}(x, y, z)$, we obtain a highly precise calculation. Therefore, highly precise positioning is maintainable by setting the obtained valued of $\mathrm{Rx}(x, y, z)$ to b $\mathrm{Rx}_0(x_0, y_0, z_0)$ in the subsequent calculation.

V. Behavior of Our Positioning Hardware

A. Signal Generation and Transmission on a Transmission unit

Fig. 7 shows the block diagram of our positioning system. The signal or value, processing and device are plotted as solid, dashed and double lines, respectively. In this system, the transmission unit shown in Fig. 7 (a) consists of a FPGA (Cyclone EP1C6Q240C6, Altera), a wireless module (single chip 2.4 GHz transceiver nRF24L01, Nordic Semiconductor), an amplifier, and 4 transmitters (PC40-18S, Nippon Ceramic). The transmission unit operates at a frequency of 100 MHz. An SS signal is generated continuously by carrier waves at a frequency of 40 kHz and the MLS is obtained using a 9-bit shift register in FPGA mounted on the transmission unit (see Fig. 7 (b)). The transmission volume of the SS signal can be amplified up to 10.5 Vp-p. We utilize an ultrasonic transmitter with a closed-type aperture. Fig. 8 shows directivity of this transmitter. The beam half angle of the transmitter shown in Fig. 8 is approximately 80 degrees. Transmission start timing is sent by the wireless module as radio waves. The timing is set in the 20 periods of MLS because a reception unit needs a long interval to perform simultaneously synchronization of a sampling frequency and transmission timing using the same radio waves.

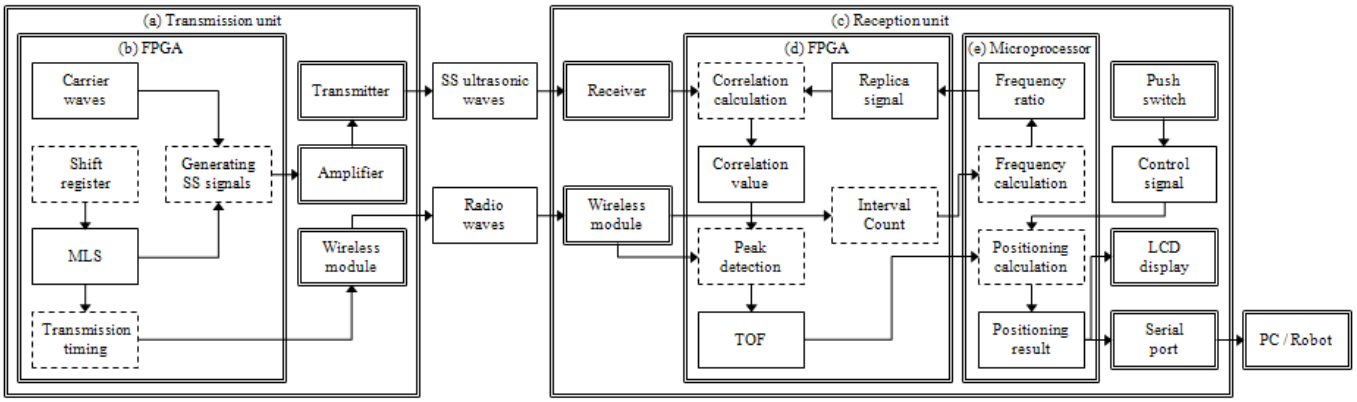

Fig. 7 The block diagram of our positioning system, (a) a transmission unit consists of (b) FPGA, a wireless module, an amplifier and 4 transmitters; (c) a reception unit consists of (d) FPGA, wireless module, (e) a microprocessor, a receiver, 4 push switches, a serial port and a LCD display

B. *Signal Detection and Positioning Calculation in Reception Unit*

The reception unit shown in Fig. 7 (c) consists of a FPGA (same as the transmission unit), a wireless module (same as the transmission unit), a microprocessor (AKI-H8/3052F, Akizuki Densi Tsusho), a receiver ("Mini" SiSonic Ultrasonic Acoustic Sensor SPM0404UD5, Knowles Electronics), 4 push switches, a serial port, and a LCD display. The reception unit also operates at a frequency of 100 MHz. Transmitted SS ultrasonic waves are acquired using the receiver with Omni-directional characteristics, and the bandwidth is flat from 10 to 65 kHz. In FPGA mounted on the reception unit, a correlation value is calculated in 6.25 µs interval using the received and replica signals shown in Fig. 7 (d). The TOF is obtained from the peak of the correlation value and transmission timing, and is received by wireless module with radio waves. More than 3 TOF values that are obtained simultaneously are sent to the microprocessor in 16-bit widths. In addition the frequency ratios between transmission and reception units are calculated and sent to FPGA. The microprocessor operates at 25 MHz. The positioning calculation result is sent to an LCD display and a serial port which allows for communication between an autonomous robot and our system.

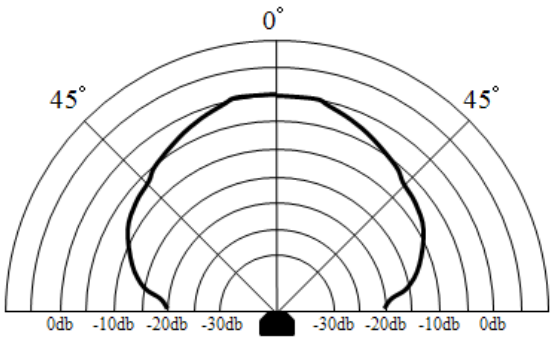

Fig. 8 The schematic of directivity of a transmitter, which has directivity of 80 degrees

A real-time operating system is installed on the microprocessor (TOPPERS/JSP, TOPPERS Project). It can execute plural software by time-sharing in parallel and can therefore simultaneously calculate a position and frequency. Multiplication and division of decimal fractions are processed quickly using fixed-point arithmetic.

VI. Measurement Precision Using Simultaneous Transmission and Reception by 4 Channels CDMA

A. *Experimental Outline for Measuring Distance*

The measurement precision might be degraded at the CDMA, when compared to single channels, as a result of other signals registering as noise. We therefore conducted an experiment to investigate the measurement precision simultaneously using 4 channels of the CDMA, as shown in Fig. 9. 4 transmitters, Tx_1, Tx_2, Tx_3, and Tx_4, are installed in arc line at intervals of 160 mm. The transmitters and the transmission unit were connected using a 3.5 mm phone connector cable and the transmission volume was adjusted to 10.5 Vp-p.

A receiver was mounted at the center of the arc where the transmitters were installed for equalizing distance between transmitters and a receiver. The transmission timing was sent via cable to evaluate the influence of the errors induced by the CDMA. We measured 1000 mm intervals at 1000 to 6000 mm using a receiver. The experiment was conducted 10 times at the each distance and the results were evaluated using the Root Mean Squared (RMS) of difference between the results and the installed distances. The RMS error em is defined as

$$\sqrt{(} \qquad (24)$$

Here, d_i is the measured distance and is the true distance between a receiver and i-th transmitter. The average value of the RMS measurement error is discussed below.

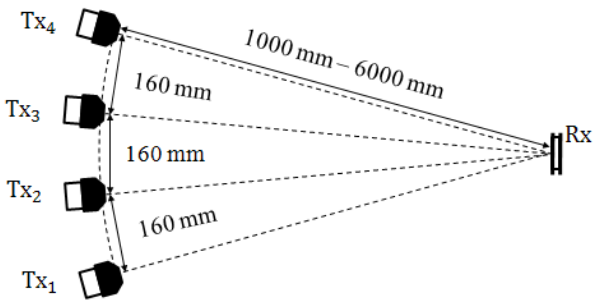

Fig. 9 Experimental outline of a measurement distance for revealing precision at 4 channels CDMA

B. *Experimental Result on Measuring Distance at CDMA*

Fig. 11 shows the measurement error when 4 channels of the CDMA are used, when compared with the use of only 1 channel. The vertical and horizontal axes correspond to the measurement error and measurement distance, respectively. The bars show the RMS values for the 4 channel experiment and the dotted line shows the 1 channel experiment.

Generally, the measurement precision is decreased using 4 channels, when compared to using only 1 channel. The average error when using only 1 channel was 15 mm, whereas the average errors Tx_1, Tx_2, Tx_3, and Tx_4 using CDMA were 19, 20, 34 and 25 mm, respectively. The largest error measured was 38 mm, when Tx_2 was at a distance of 6000 mm. On average the error when using 4 channels increased by a factor of 1.7, when compared to using 1 channel. Further, when the distances are shorter the errors increased. Thus, we conclude that signals from different channels contribute to the noise and degrade the measurement precision. This suggests that, even though a MLS with low cross-correlation was used, the precision decreases. However, the measurement precision was below 50 mm for distances of 1000 to 6000 mm.

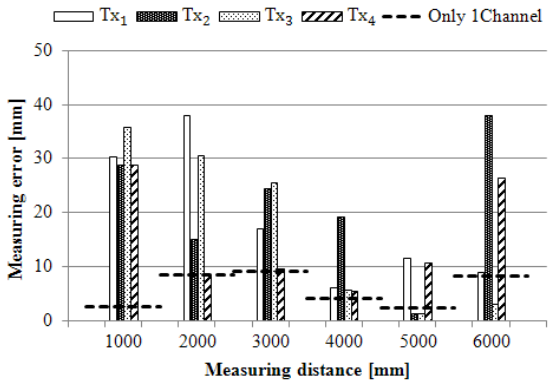

Fig. 11 RMS errors using 4 channels of the CDMA, compared with only 1 channel

VII. Positioning Experiment Using Continuous Signals

A. *Experimental Outline for Positioning Using Continuous Signals*

Experiments to examine the positioning accuracy of the positioning system using continuous signals and calculation algorithm based on Newton–Raphson method were also conducted, as shown in Fig. 10. A given experimental space has 4 transmitters, Tx_1, Tx_2, Tx_3, and Tx_4, installed in the corners of a 4000 mm rectangular and directed toward the center of area, (2000, 2000, 0) mm. The heights of Tx_1 to were measured using a laser range finder since the height the floor to the roof differed over the area of the experiment. Their heights were 2632, 2627, 2639 and 2626 mm, respectively. The same connection method (between the transmission unit and a transmitter, and between a reception unit and a receiver), and transmission volume was used. Fig. 10 (b) shows the measurement positions.

We measured at 49 points with receiver heights of 500, 1000 and 1500 mm (assumed to be average heights of robots), respectively (see Fig. 10 (a)). The receiver and the reception unit were connected using the same cable that connected the transmitters and the transmission unit. The positioning experiment was conducted 20 times at each of the 49 points, respectively. The experimental results were evaluated using the RMS as above. As such, the positioning error ep_{rms} is defined using the measured distances x_m, y_m, and true distances x, y, z, corresponding to each coordinate:

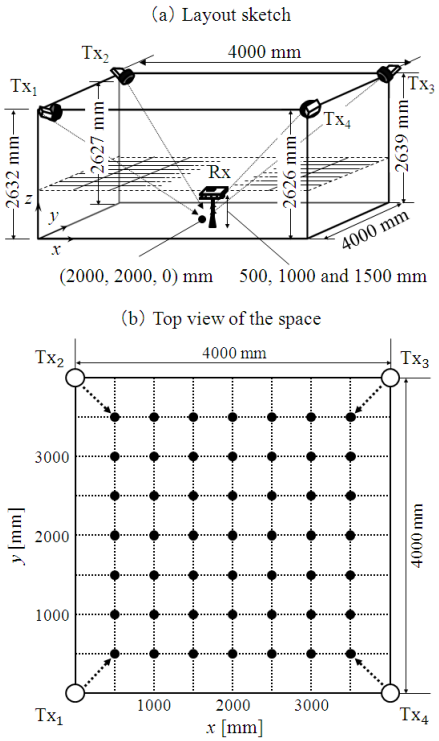

Fig. 10 Outline of a positioning experimental environment

$$\sqrt{(} \quad (25)$$

The average value of the RMS is defined as the positioning error at each point. The positioning error and calculation time are discussed as factors relating to the usefulness of the system.

B. *Experimental Results and Discussion of the Positioning Experiment*

Fig. 12 shows a top view of the positioning accuracy for measurement points. Fig. 12 (a), (b) and (c) show the positioning accuracy at for receiver heights of $h = 500$, 1000 and 1500 mm, respectively. The scale at the top shows the range for a positioning error at each measurement point. For example, the ① corresponds to a range of positioning errors between 0 mm through 10 mm.

From this experiment, the average positioning errors from all measurement points was 31 mm, with respective averages of 30, 35 and 27 mm at h =500, 1000 and 1500 mm, respectively.

Moreover, the standard deviations were 6, 7 and 7 mm, respectively, and the probabilities of positioning errors being within 30 mm were 49, 22 and 63 %. This suggests that the receiver at a height of 1000 mm gave rise to the worst precision. While small distances give rise to interference errors, we suspect that this is due to the directivities of and angle settings of the transmitter. However, the standard deviations show that the positioning error is uniform over the positioning space. Although greater measurement errors are obtained using simultaneous CDMA and continuous signals, when compared to conventional TDMA, the measurement errors at each positioning point was less than 50 mm.

TABLE I shows the maximum, minimum and average times of calculation using the proposed method. The response time-cycle, which is an interval from the arrival of the electrical signal to the positioning acquisition, is also given. As such, the response period contains the calculation period. The maximum, minimum and average times of the calculation time were 17, 11 and 14 ms, respectively. That is, the proposed method can calculate positions in less than 20 ms. Moreover, the maximum, minimum and average times of response were 72, 56 and 65 ms. Therefore, we can obtain a position in a response time of less than 80 ms, even though we use a relatively slow H8 processor. This is within the requirements for the self-localization of autonomous robots (<100 ms). From the above accuracy and response time results, we conclude that the proposed system could be used for the self-localization of autonomous robots.

TABLE I THE MAXIMUM, MINIMUM AND AVERAGE TIME OF CALCULATION AND RESPONSE

	Maximum [ms]	**Minimum [ms]**	**Average [ms]**
Calculation time	15	11	12
Response time	72	56	65

VIII. CONCLUSION

In this paper, the positioning accuracies and response times were verified using real-time positioning with a CDMA and continuous SS ultrasonic waves. For measurements using continuous signals, we proposed a calculation algorithm based on the Newton–Raphson method, in analogy to GNSS.

In the proposed system the transmission start timing is synchronized every 20 periods of MLS. The transmission start timing is used for the synchronization of a sampling frequency between a transmission unit and a reception unit. For signal detection of SS ultrasonic waves, the reception unit continues calculating a correlation value from a received signal and a replica signal using a sum-of-products operation. The distance between a transmitter and a receiver is acquired using TOF, obtained from the difference between the peak and transmission start times. A position is obtained using more than 3 distances and the TOF. The proposed method calculates results with high accuracy by inserting the

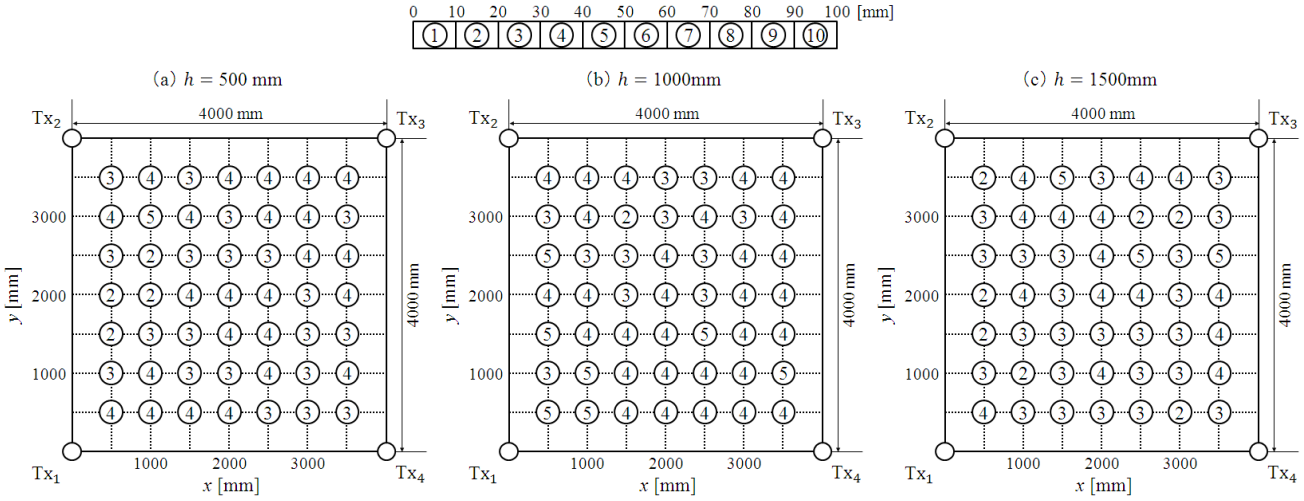

Fig. 12 Distribution of positioning errors at the receiver height (a) 500 mm, (b) 1000 mm, (c) 1500 mm

previous position into the subsequent calculation.

We analyzed the efficacy of using CDMA with 4 channels to accurately measure distances. The interference of incoming signals was confirmed. Moreover, when the distance between transmitters and receivers was in the range of 1000 to 6000 mm, the measurement errors using 4 channels was a factor of 1.7 times greater than using 1 channel. However, at all distances measured the errors were less than 50 mm, showing that the system has enough measurement accuracy for positioning.

A positioning experiment using the proposed algorithm confirmed its efficacy. The positioning accuracy and response time was discussed. We found that the accuracy was almost uniform over a 4000 mm by 4000 mm square space, although this accuracy was decreased by interference. The average RMS of errors was 31 mm (30, 35 and 27 mm for receiver heights of 500, 1000 and 1500 mm, respectively): values less than 50 mm. Moreover, the average time of calculation and response were 12 ms and 65 ms, respectively. This suggests our system using CDMA has sufficient accuracy and real-time properties.

In the future we will discuss the feasibility of the 3D self-localization of autonomous mobile robots, using a radio controlled helicopter to experiment with moving targets [9].

REFERENCES

[1] M. Ishii, M. Asako, K. Okano, H, Torimoto, K. Suzuki, I. Petrovsky, “Pseudelite Application for ITS,” IEIC Technical Report, Vol.104, No.230, pp.13-18, July 2004.

[2] D. Manandhar, H. Torimoto, “Development of IMES Installation, Setup and Management System,” in Proceedings of the 24th International Technical Meeting of The Satellite Division of the Institute of Navigation, Portland, pp.1507-1513, 2011.

[3] A. Sanchez, S. Elvira, A. de Castro, G. Glez-de-Rivera, R. Ribalda, J. Garrido, “Low cost indoor ultrasonic positioning implemented in FPGA,” in Industrial Electronics Conference (IECON 2009), Taiwan, 2009.

[4] H. Mike，H. Andy, “Broadband Ultrasonic Location Systems for Improved Indoor Positioning,” IEEE Trans Mob Compt, pp.536-547, 2006.

[5] A. Yamane, T. Iyoda, Y. Chio, Y. Kubota, K. Watanabe, “A Study on Propagation Characteristics of Spread Spectrum Sound Waves using a Band-limited Ultrasonic Transducer,” Journal of Robotics and Mechatronics, Vol.16, No.3, pp.333-341, 2004.

[6] A. Suzuki, T. Iyota, “Angular Dependence of Transducers for Indoor Positioning System Using SS Ultrasonic Waves,” in International Conference on Indoor Positioning and Indoor Navigation (IPIN 2012), Sydney, pp.CD-ROM, 2012.

[7] A. Suzuki, T. Iyota, Y. Choi, Y. Kubota, K. Watanabe, A. Yamane, “Measurement Accuracy on Indoor Positioning System Using Spread Spectrum Ultrasonic Waves,” in 4th International Conference on Autonomous Robots and Agents, Wellington, New Zealand, pp.294-297, 2009.

[8] A. Suzuki, T. Iyota, K. Watanabe, “Real-Time Distance Measurement for Indoor Positioning System Using Spread Spectrum Ultrasonic Waves,” in Ultrasonic Waves. University Campus STeP Ri Slavka Krautzeka 83/A 51000, Rijeka, Croatia, INTECH, pp.173-188, 2012.

[9] Y. Itagaki, A. Suzuki, T. Iyota, “Indoor Positioning for Moving Objects Using a Hardware Device with Spread Spectrum Ultrasonic Waves,” in International Conference on Indoor Positioning and Indoor Navigation (IPIN 2012), Sydney, pp.CD-ROM, 2012.

[10] P. Atkins, J. de Paula, “Atkins' Physical Chemistry,” Oxford University Press, 2006.

[11] P. Misra, P. Enge, “Global Positioning System Signals: Measurements, and Performance,” Ganga-Jamuna Press, 2001.

[12] W. H. Press, W. T. Vetterling, S. A. Teukolsky, B. P. Flannery, “Numerical Recipes in C,” Chapter15, pp.671-681, Cambridge University Press, 1986.